

# VLBI differential astrometry at 43 GHz

J.C. Guirado<sup>1</sup>, J.M. Marcaide<sup>1</sup>, M.A. Pérez-Torres<sup>1</sup>, and E. Ros<sup>2</sup>

<sup>1</sup> Departamento de Astronomía, Universitat de València, E-46100 Burjassot, Valencia, Spain

<sup>2</sup> Max-Planck-Institut für Radioastronomie, Auf dem Hügel 69, D-53121, Bonn, Germany

A&A, 353, L37-L40 (2000)

**Abstract.** From 43 GHz VLBA observations of the pair of radio sources QSO 1928+738 and BL 2007+777 we have demonstrated the feasibility of precision phase-delay differential astrometric techniques at millimeter wavelengths. For a pair of sources with  $5^\circ$  separation and high antenna elevations, we have shown that present astrometric models and millimeter arrays are advanced enough to model the differential phase-delay to within 2 picoseconds, less than one tenth of a phase-cycle at 43 GHz. The root-mean-square of the differential phase-delay residuals is dominated by the fluctuations of the atmospheric water vapor. We have determined the relative position of the observed sources with a precision twofold better than previous determinations at lower frequencies and, more importantly, largely free from ambiguous definitions of the reference point on the structure of the radio sources. Our result makes 43 GHz VLBI phase-delay differential astrometry an ideal tool to study the absolute kinematics of the highly variable structures of regions near the core of extragalactic radio sources.

**Key words:** astrometry – techniques: interferometric – quasars: individual: QSO 1928+738 – BL Lacertae object: individual: BL 2007+777

## 1. Introduction

One of the trends in Very-Long-Baseline Interferometry (VLBI) is to augment the angular resolution of the observations in search for a more detailed view of the inner structure of extragalactic radio sources. This is effectively carried out by either observing at millimeter wavelengths (mm-VLBI) or, at cm-wavelengths, by combining ground telescopes with antennas in space. The correct interpretation of these high-resolution observations is of much relevance since they map the morphology of highly variable regions close to the central engine of AGNs. However, multi-epoch analyses directed to understand the dynamical behavior of these inner regions critically depend

on the alignment of the images: no solid conclusions can be extracted without an accurate source component (i.e. core) identification. In particular, VLBI reveals that cm-wavelength components break up in complex structures with multiple features at mm-wavelengths. These compact mm-features show a strong variability, which may be the result of phenomena only seen so far in numerical simulations (Gómez et al. 1995). For a meaningful physical understanding of those compact features, a detailed knowledge of the (absolute) kinematics of the region is crucial. It is therefore highly desirable to extend precision differential phase-delay astrometry to mm-wavelengths. In this Letter we demonstrate the feasibility of using phase-delay differential astrometry at 43 GHz. We have selected the pair of sources QSO 1928+738 and BL 2007+777,  $\sim 5^\circ$  apart, with flat spectra, high flux densities, and rich structures at 43 GHz. The astrometry analysis of these data show the advantages and possibilities of mm-wavelength differential astrometry.

## 2. Observations and Maps

We observed the radio sources QSO 1928+738 and BL 2007+777 at 43 GHz on 1999 January 3 from 15:00 to 23:30 UT. We used the complete Very Long Baseline Array (VLBA) recording in mode 256-8-2 in left circular polarization to achieve a recording bandwidth of 64 MHz. We interleaved observations of QSO 1928+738 and BL 2007+777 using integration times between 40 and 130 seconds on each source to make total cycle time durations between 110 and 300 seconds (antenna slew time was 15 seconds). The data were correlated at the National Radio Astronomy Observatory (NRAO, Socorro, NM, USA). Detections were found on both sources to all stations but Hancock, presumably due to severe weather conditions at this site. We made manual phase calibration, visibility amplitude calibration (using system temperatures and gain curves from each antenna), and fringe fitting at the correlation position with the NRAO Astronomical Image Processing System (AIPS). For astrometric purposes, we further processed the data in AIPS (tasks MBDLY and CL2HF) to obtain, for each baseline and epoch, estimates

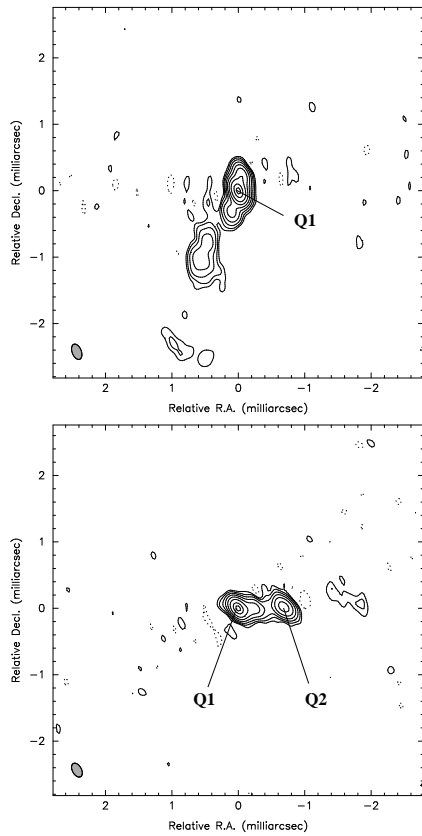


**Fig. 1.** 43 GHz hybrid maps of QSO 1928+738 (left) and BL 2007+777 (right) at epoch 1999.01. Contours are - 0.5,0.5,1,2,4,8,16,32,64, and 90% of the peak of brightness, 0.56 Jy/beam, for QSO 1928+738, and -1,1,2,4,8,16,32,64, and 90% of the peak of brightness, 0.22 Jy/beam, for BL 2007+777. The restoring beam (shown at the bottom left corner of each map) is an elliptical Gaussian of  $0.24 \times 0.14$  mas (P.A.  $21^\circ$ ) for QSO 1928+738, and  $0.23 \times 0.14$  mas (P.A.  $29^\circ$ ) for BL 2007+777. The astrometric reference points are labeled as Q1, and correspond to the peak of brightness of each map. See text.

of the group delay, phase-delay rate, and fringe phase at a reference frequency of 43,185 MHz. We discarded data from Saint Croix and Pie Town stations, which showed unacceptable scatter in the observables, for the astrometric analysis presented in Sect. 3. For mapping purposes, we transferred the data into the Caltech imaging program DIFMAP (Shepherd et al. 1995). We performed several iterations of self-calibration in phase and gain. We present the resulting hybrid maps in Fig. 1.

The 43 GHz map of QSO 1928+738 displays several jet components extending southwards. All these features appear blended together as only one or two components in previous maps at cm-wavelengths (Guirado et al. 1995, hereafter G95; Ros et al. 1999, hereafter R99), and those obtained with space VLBI (Murphy et al. 1999). The brightest knot, labeled as Q1, is probably a jet component, unless the source is two-sided, but it is compact and

well defined. Thus, it constitutes an appropriate reference point for relative astrometry at a single epoch. However, this component would not be a suitable reference point for a multi-epoch comparison of the relative separation between the two sources as it is likely to move and evolve in brightness and shape over time.

The 43 GHz map of BL 2007+777 represents a significant improvement in the knowledge of the inner structure of this source (see Fig. 1). The brightest knot seen earlier at cm-wavelengths (Guirado et al. 1998, hereafter G98; R99) breaks-up in at least three new features. The kinematic nature of component Q2, almost as bright as the easternmost component Q1, is of much interest. The brightest feature of BL 2007+777 at cm-wavelengths, a blending of all components seen within 1 mas from the origin in our 43 GHz map, has been taken as a reference point for astrometry (G95; G98; R99); even more, this feature has been considered stationary for multi-epoch astrometry analyses. Accordingly, should component Q2 be a travelling knot, the selected reference point at cm-wavelengths is likely to be not stable over time and part of previous astrometry results must be revised.

### 3. Astrometry Analysis

A goal of this research has been to calibrate the limitations of our standard astrometry procedure for 43 GHz, as well as to study the potential precision of the astrometric data at this frequency. Therefore, the data-reduction procedure for the 43 GHz observation deliberately followed the same steps as those used for the 5 GHz (G95) or 8.4 GHz observations (G98; R99). We briefly go again over each step of this analysis: For our 43 GHz data, (i) we predicted, via a precise theoretical model of the geometry of the array and the propagation medium, the number of cycles of phase between consecutive observations of the same source to permit us to “connect” the phase delay (e.g. Shapiro et al. 1979; G95; R99); (ii) we defined as reference points in the 43 GHz images of the two radio sources the maximum of the brightness distribution (components Q1 in the maps of QSO 1928+738 and BL 2007+777; see Fig. 1) and subtract the contribution of the structure of the radiosources, with respect to the reference points selected, from the phase delays; (iii) we formed the differenced phase delays by subtracting the residual (observed minus theoretical values) phase delay of BL 2007+777 from the previous observation of QSO 1928+738; and (iv) we estimated the relative position of the reference points from a weighted-least-squares analysis of the differenced residual phase delays. For this analysis we used an improved version of the program VLBI3 (Robertson 1975).

In step (i), the geometry of our theoretical model (set of antenna coordinates, Earth-orientation parameters, and source coordinates) was consistently taken from IERS (IERS 1998 Annual Report, 1999). The theoretical model also accounted for the effect of the propagation medium

**Table 1.** Contributions to the standard errors of the estimates of the coordinates of QSO 1928+738 minus those of BL 2007+777 ( $\delta\Delta\alpha$ ,  $\delta\Delta\delta$ ) from the sensitivity study.

Effect		Standard Deviation <sup>a</sup>	$\delta\Delta\alpha^b$ ( $\mu\text{s}$ )	$\delta\Delta\delta$ ( $\mu\text{as}$ )
Statistical errors <sup>c</sup>		–	4	25
Ref. point identification		–	0.6	1
Station coordinates		2 cm	6	25
Coordinates of BL 2007+777:	$\alpha$	100 $\mu\text{s}$	23	41
Earth’s pole:	$\delta$	300 $\mu\text{as}$	9	9
	$x$	150 $\mu\text{as}$	2	9
	$y$	250 $\mu\text{as}$	2	4
UT1-UTC		15 $\mu\text{s}$	3	5
Earth’s nutation:	$d\psi$	170 $\mu\text{as}$	0.3	1
	$d\epsilon$	80 $\mu\text{as}$	1	2
Ionosphere <sup>d</sup>		1 TECU	1	2
rss <sup>e</sup>			26	56

<sup>a</sup> The standard deviation of the fixed geometrical parameters of our astrometric model (all entries but ionosphere) were taken from IERS Annual Report 1998 (1999). The 2 cm standard deviation of the site coordinates corresponds to each of the three coordinates for each antenna site.

<sup>b</sup> Notice that the values of  $\delta\Delta\alpha$  are in  $\mu\text{s}$ . To convert  $\mu\text{s}$  to  $\mu\text{as}$ , the factor  $15 \cdot \cos \delta_{\text{QSO } 1928+738}$  ( $\sim 4.2$ ) must be used.

<sup>c</sup> The statistical errors include the uncertainties of the tropospheric zenith delays at the nodes of the piecewise linear function used in the troposphere model (see Sect. 2).

<sup>d</sup> Standard deviation provided by the global ionospheric maps at each site. 1 TECU =  $1 \times 10^{16}$  el m<sup>-2</sup>.

<sup>e</sup> Root-sum-square of the tabulated values.

in the astrometric observables. We modeled the ionospheric delay by using total electron content (TEC) data from GPS-based global ionospheric maps generated at the epoch of our observations by the Center for Orbit Determination in Europe (Schaer et al. 1998). We followed the geometric corrections described in Klobuchar (1975) and Ros et al. (2000). We modeled the tropospheric zenith delay at each station as a piecewise-linear function characterized by values specified at epochs one hour apart. We calculated a priori values at these nodes from local surface temperature, pressure, and humidity, based on the model of Saastamoinen (1973). The antenna elevations were always higher than 20° at all stations; this allowed us to use the dry and wet Chao mapping functions (Chao 1974) to determine the tropospheric delay at non-zenith elevations for each observation at each site. We estimated the tropospheric zenith delay at the nodes of each station, along with the relative position of the sources, from a weighted-least-squares analysis.

#### 4. Results and Discussion

From the astrometric analysis described in Sect. 3, we obtain the following J2000.0 coordinates of QSO 1928+738 minus those of BL 2007+777 at 43 GHz:

$$\begin{aligned} \Delta\alpha &= -0^h 37^m 42^s 503443 \pm 0^s 000026 \\ \Delta\delta &= -3^\circ 54' 41'' 677208 \pm 0'' 000056 \end{aligned}$$

where the quoted uncertainties are overall standard errors (see Table 1), nearly twofold smaller than the standard errors corresponding to previous determinations at 5 and 8.4 GHz. From the comparison of the results of the sensitivity analysis displayed in Table 1 with similar sensitivity analyses at lower frequencies (G95; R99), we see that the improvement in precision comes from (i) the small contribution to the standard errors of the reference point identification in the map (dominated by image noise), as a consequence of the improvement of resolution of the maps and of the lack of ambiguity in selecting the components acting as reference, and (ii) the negligible contribution of the ionosphere, that scales down by a factor of 25 with respect to its contribution at 8.4 GHz. As occurs at cm-wavelengths, the quoted standard errors of the relative position are dominated by the uncertainties of the fixed parameters of the astrometric model (entries 3 to 10 of Table 1), and, in particular, by the uncertainties of the coordinates of the reference source, as expected for objects with a large angular separation (notice that this error is not frequency dependent). The comparison and interpretation of the relative position estimate at 43 GHz with previously reported estimates at lower frequencies will be postponed to a later publication where the comparison will be made in great detail.

The postfit residuals of the differenced phase delays corresponding to all baselines included in our analysis are shown in Fig. 2. Note the scale of the plots,  $\pm 23$  ps, corresponding to  $\pm 1$  phase cycle. The average root-mean-square (rms) of the postfit residuals is 2 ps, less than one tenth of the phase cycle at 43 GHz. At this level of precision, the absence of systematic effects validates both the astrometric model, based on IERS standards, and the propagation medium procedures for mm-wavelength VLBI astrometry (at least for cycle times, source separations, weather conditions, and antenna elevations similar to those presented in this paper). To calibrate the quality of our procedure, we compared the residual of the differenced phase delay with similar residuals corresponding to observations at 8.4 GHz and 5 GHz made in the past (G95, G98). The rms of the residuals are about 15, 9, and 2 ps for the data sets at 5, 8.4, and 43 GHz, respectively, which expressed in equivalent-phase yield postfit residuals of roughly 30 degrees at each of the three frequencies. This similarity of the rms expressed in phase at all the observed frequencies demonstrates not only that the phase connection process is feasible at 43 GHz, but which is also of no less quality than at lower frequencies.

Likely, the most important contributors to the scatter of the phases at 43 GHz are the unmodeled variations of the refractivity of the neutral atmosphere. From the average rms of 2 ps of the phase residuals of Fig. 2, and assuming uncorrelated contributions from the antennas forming

each interferometric pair, the average uncertainty for the single-site phase delay is  $\sqrt{2}$  ps. This uncertainty is in good agreement with the predictions of water vapor fluctuations on time scales of 100 seconds ( $\sim 2$  ps) based on refractivity patterns described by Kolmogorov turbulences (Treuhaft & Lanyi 1987).

The importance of our result translates to VLBI phase-referencing mapping. This technique (see e.g. Lestrade et al. 1990) relies completely on the behavior of the phase of the reference source (usually a strong radio emitter) to predict the phase of the target source (usually a weak radio emitter). Beasley & Conway (1995) provide useful expressions for the maximum cycle time for phase-referencing with the VLBA. Under good weather conditions, average antenna elevation of  $40^\circ$ , and with the requirement that the rms phase between scans is  $<90^\circ$ , the maximum cycle time at 43 GHz is  $\sim 100$ s. This estimate should be shortened if atmospheric spatial variations from different lines of sight are considered. Actually, the facts are more favorable. For sources separated  $5^\circ$  on the sky, high antenna elevations, and good weather conditions, our results show that (i) the rms of the phases is below  $90^\circ$  throughout the experiment and does not seem to be substantially dependent of the cycle times used during our observation (100-300s); and (ii) the expected average uncertainty in interpolating the phases of one source to the epoch of the other is  $\sim 30^\circ$  in the differenced phase. This value is not larger than usual phase errors in phase-reference mapping at cm-wavelengths (e.g. Lestrade et al. 1990). Therefore, with the proper cycle times and nearby calibrator sources, diffraction limited VLBI phase-reference images at 43 GHz should be possible.

Our observations have shown that VLBI differential astrometry at 43 GHz provides high-precision relative positions. At this frequency, the astrometric precision is nearly equivalent to the resolution of the maps, and the reference point selected in the source structure might be associated with the core. This makes 43 GHz differential astrometry an ideal technique to trace unambiguously the kinematics of the inner regions of the extragalactic radiosources.

*Acknowledgements.* We thank Patrick Charlot for a constructive refereeing of the paper and Walter Alef for his valuable comments. We thank Jon Romney for his efforts during the correlation. This work has been supported by the Spanish DG-ICYT grant PB96-0782. The National Radio Astronomy Observatory is operated by Associated Universities Inc., under a cooperative agreement with the National Science Foundation.

## References

Beasley A.J., Conway J.E., 1995, In: Zensus J.A., Diamond P.J., Napier P.J. (eds.), Very Long Baseline Interferometry and the VLBA, ASP Conference Series 82, San Francisco, CA, USA, p. 327  
 Chao C.C., 1974, JPL/NASA Tech. Rep. No. 32-1587, 61  
 Gómez J.L., Martí J.M., Marscher, A.P., et al., 1995, ApJ 449, L19

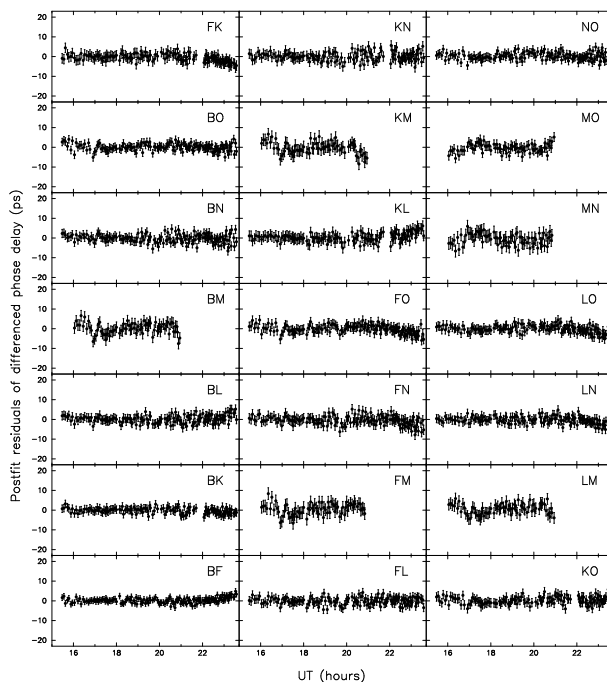


**Fig. 2.** Postfit residuals of the difference phase delays at 43 GHz for all baselines. Full vertical scale is  $\pm$ one phase cycle ( $\pm 2\pi$  equivalent), i.e.,  $\pm 23$  ps. The average rms is 2 ps, less than one tenth of a phase cycle at 43 GHz. The symbols correspond to the following VLBA antennas: B, Brewster; F, Fort Davis; K, Kitt Peak; L, Los Alamos; M, Mauna Kea; N, North Liberty; O, Owens Valley

Guirado J.C., Marcaide J.M., Elósegui P., et al., 1995, A&A 293, 613 [G95]  
 Guirado J.C., Marcaide J.M., Ros E., et al., 1998, A&A 336, 385 [G98]  
 International Earth Rotation Service (IERS), 1999, Annual Report for 1998, Gambis, D. (ed.), Observatoire de Paris, France  
 Klobuchar J.A., 1975, Air Force Cambridge Research Laboratories Report No. AFCRL-TR-75-0502 (NTIS ADA 018862)  
 Lestrade J.F., Rogers, A.E.E., Whitney, A.R., et al., 1990, AJ 99, 1663  
 Murphy, D.W., Tingay S.J., Preston R.A., et al., 1999, New Astronomy Reviews 43, 727  
 Robertson D.S., 1975, Ph.D. Thesis, Massachusetts Institute of Technology, Cambridge, MA, USA  
 Ros E., Marcaide J.M., Guirado J.C., et al., 1999, A&A 348, 381 [R99]  
 Ros E., Marcaide J.M., Guirado J.C., et al., 2000, A&A submitted  
 Saastamoinen J., 1973, Bull. Géodésique 105, 279  
 Schaer S., Gurtner W., Feltens J., 1998, In: Proceedings of the IGS AC Workshop, Darmstadt, Germany: <http://www.cx.unibe.ch/aiub/ionosphere.html>  
 Shapiro I.I., Wittels J.J., Counselman C.C., et al., 1979, AJ 84, 1459  
 Shepherd M.C., Pearson T.J., Taylor G.B., 1995, BAAS 26, 987

Treuhaf R.N., Lanyi G.E., 1987, Radio Science 22, 251